

MCLMR: A Model-Agnostic Causal Learning Framework for Multi-Behavior Recommendation

Ranxu Zhang

School of Artificial Intelligence and
Data Science, University of Science
and Technology of China
Hefei, China
zkd_zrx@mail.ustc.edu.cn

Junjie Meng

School of Artificial Intelligence and
Data Science, University of Science
and Technology of China
Hefei, China
mengjre@gmail.com

Ying Sun

Artificial Intelligence Thrust, The
Hong Kong University of Science and
Technology (Guangzhou)
Guangzhou, China
sunyinggilly@gmail.com

Ziqi Xu

RMIT University
Melbourne, Australia
ziqi.xu@rmit.edu.au

Bing Yin

State Key Laboratory of Cognitive
Intelligence
iFLYTEK Research, iFLYTEK
Hefei, China
bingyin@iflytek.com

Hao Li

iFLYTEK Research, iFLYTEK
Hefei, China
haoli5@iflytek.com

Yanyong Zhang

School of Artificial Intelligence and
Data Science, University of Science
and Technology of China
Hefei, China
yanyongz@ustc.edu.cn

Chao Wang*

School of Artificial Intelligence and
Data Science, University of Science
and Technology of China
State Key Laboratory of Cognitive
Intelligence
Hefei, China
wangchaoai@ustc.edu.cn

Abstract

Multi-Behavior Recommendation (MBR) leverages multiple user interaction types (e.g., views, clicks, purchases) to enrich preference modeling and alleviate data sparsity issues in traditional single-behavior approaches. However, existing MBR methods face fundamental challenges: they lack principled frameworks to model complex confounding effects from user behavioral habits and item multi-behavior distributions, struggle with effective aggregation of heterogeneous auxiliary behaviors, and fail to align behavioral representations across semantic gaps while accounting for bias distortions. To address these limitations, we propose MCLMR, a novel model-agnostic causal learning framework that can be seamlessly integrated into various MBR architectures. MCLMR first constructs a causal graph to model confounding effects and performs interventions for unbiased preference estimation. Under this causal framework, it employs an Adaptive Aggregation module based on Mixture-of-Experts to dynamically fuse auxiliary behavior information and a Bias-aware Contrastive Learning module to align cross-behavior representations in a bias-aware manner. Extensive experiments on three real-world datasets demonstrate that MCLMR achieves significant performance improvements

*Chao Wang is the corresponding author.



This work is licensed under a Creative Commons Attribution 4.0 International License.
WWW '26, Dubai, United Arab Emirates
© 2026 Copyright held by the owner/author(s).
ACM ISBN 979-8-4007-2307-0/2026/04
<https://doi.org/10.1145/3774904.3792495>

across various baseline models, validating its effectiveness and generality. All data and code will be made publicly available. For anonymous review, our code is available at the following link: <https://github.com/gitrxh/MCLMR>.

CCS Concepts

• **Information systems** → **Recommender systems**; • **Computing methodologies** → *Causal reasoning and diagnostics*.

Keywords

Recommender Systems, Causal Intervention, Multi-behavior.

ACM Reference Format:

Ranxu Zhang, Junjie Meng, Ying Sun, Ziqi Xu, Bing Yin, Hao Li, Yanyong Zhang, and Chao Wang. 2026. MCLMR: A Model-Agnostic Causal Learning Framework for Multi-Behavior Recommendation. In *Proceedings of the ACM Web Conference 2026 (WWW '26)*, April 13–17, 2026, Dubai, United Arab Emirates. ACM, New York, NY, USA, 12 pages. <https://doi.org/10.1145/3774904.3792495>

1 Introduction

Recommender systems [10, 12, 28, 30] are essential for information discovery. While Traditional Collaborative Filtering (CF) [11, 25, 27, 31] effectively models preferences, it typically relies on single-behavior data, causing data sparsity. Multi-Behavior Recommendation (MBR) [8, 13, 36] addresses this by leveraging diverse interactions (e.g., views, clicks) to enrich preference modeling. However, existing MBR approaches face a fundamental challenge: multi-behavior data inherently contains multi-behavior biases, where

different users exhibit distinct behavioral patterns and different items receive varying behavior type distributions. Ignoring such bias modeling leads to suboptimal preference learning and compromised recommendation quality.

To leverage multiple behaviors, researchers have proposed various MBR approaches. Early methods like CMF [48] employ matrix factorization to learn shared representations across behaviors. Recently, Graph Neural Network (GNN)-based models have become mainstream, with MBGCN [13] propagating information through behavior-specific layers and CRGCN [40] designing cascaded networks to model behavioral dependencies. However, these methods primarily focus on capturing behavioral correlations while overlooking multi-behavior biases. Meanwhile, traditional debiasing methods address single-behavior scenarios through techniques like Inverse Propensity Scoring (IPS) or causal inference to mitigate popularity bias [6] and exposure bias [1, 21]. Recent efforts have extended causal reasoning to multi-behavior settings: CVID [7] employs diffusion models to infer latent confounders, while CMSR [18] constructs causal graphs to model behavioral dependencies. Nevertheless, these approaches either lack explicit structural modeling of inter-behavior causality or insufficiently capture the dual confounding effects from both user behavioral habits and item multi-behavior distributions. How to systematically disentangle these multi-faceted biases remains an open challenge.

Hence, we identify three key challenges for multi-behavior debiasing. First, complex confounding behavioral interaction tendencies exist where popularity intertwines with behavior-specific biases (e.g., popular items attract more views regardless of preference). Second, heterogeneous behavioral patterns require dynamic aggregation, as auxiliary behaviors vary in informativeness for specific user-item pairs. Third, significant semantic gaps and bias distortions hinder effective cross-behavior representation alignment. Effectively aligning these behavioral representations in a bias-aware manner while preserving distinct semantic meanings is crucial.

Based on the above considerations, we propose a novel, model-agnostic causal learning framework for multi-behavior recommendation, named **MCLMR**, which is designed as a universal plugin to enhance existing MBRs models. Specifically, we first construct a causal graph to model the complex confounding effects in multi-behavior data and derive unbiased preference estimation through causal intervention. Under this causal framework, MCLMR addresses the remaining two challenges through: (1) an **Adaptive Aggregation module** based on a Mixture-of-Experts (MoE) architecture, which dynamically learns to fuse information from heterogeneous auxiliary behaviors in a user-item-specific manner to maximize positive transfer and suppress negative transfer; and (2) a **Bias-aware Contrastive Learning module** that employs a novel user-item dual alignment strategy to align preference representations across behavioral spaces while accounting for the distortion caused by biases. Our main contributions are as follows:

- We propose **MCLMR**, a novel model-agnostic causal framework that can be seamlessly integrated into various MBRs architectures to enhance their performance.
- We construct a causal graph to model confounding effects in multi-behavior data and derive principled intervention strategies for unbiased preference estimation.

- We design an Adaptive Aggregation module based on MoE architecture to dynamically fuse auxiliary behavior information and a Bias-aware Contrastive Learning module to align cross-behavior representations.
- Extensive experiments on three public datasets validate the superiority of our framework and the effectiveness of each core component.

2 Related Work

2.1 Multi-behavior Recommendation

Multi-behavior Recommendation (MBR) [20, 33, 39] integrates diverse interactions to alleviate target behavior sparsity. Early methods like CMF [48] jointly factorized behavior matrices via shared latent factors. Recently, GNN-based models [29] have become dominant. MBGCN [13] learns behavior strength by propagating information on a unified heterogeneous graph, while CRGCN [40] employs a cascaded GCN structure to model sequential dependencies and refine preferences. However, MBGCN often overlooks the semantic gap between behaviors, and CRGCN models raw interactions directly. Most existing methods fail to explicitly address the inherent behavioral biases that confound true user intent.

2.2 Debaised Recommendation

Debaised recommendation [5, 17, 19, 44] addresses biases caused by feedback loops. Inverse Propensity Scoring (IPS) [3] is a common technique; Multi-IPW and Multi-DR [45] extend IPS to multi-behavior scenarios, though they often require normalization (SNIPS) to mitigate high variance. Causal inference [15, 32, 37, 38] offers a deeper approach. Methods like PDA [46], Cause [2], and MACR [34] use causal intervention to handle popularity bias, while DCCL [47] employs contrastive learning to disentangle interest from conformity. To extend causal reasoning [16] to MBR, CVID [7] infers latent confounders via diffusion models [49], and CMSR [18] uses causal graphs to model behavioral dependencies. However, CVID lacks explicit structural modeling of inter-behavior causality, while CMSR insufficiently captures complex unobserved confounders. Effectively handling both within a unified framework remains an open challenge, which is the core issue this paper aims to address.

3 Preliminaries

Basic Notations. In our framework, we denote the set of users as $U = \{u_1, u_2, \dots, u_M\}$ and the set of items as $V = \{v_1, v_2, \dots, v_N\}$, where M and N are the total number of users and items, respectively.

Multi-Behavior Interaction Data. We consider K behavior types with inherent sequential dependencies (e.g., from 'view' to 'cart', then 'purchase'). The user interaction data forms a set of interaction subgraphs $\mathcal{G} = \{\mathcal{G}_1, \dots, \mathcal{G}_K\}$, where each \mathcal{G}_k contains all observed interactions for behavior type k . We explicitly define the final behavior K_t (e.g., 'purchase') as the **target behavior**, which is the ultimate prediction goal. The preceding behaviors $\{1, \dots, K_t - 1\}$ serve as auxiliary behaviors to enhance the target prediction.

Model-Agnostic Setting and Embeddings. Designed as a model-agnostic module, our framework can be integrated with any backbone multi-behavior model (e.g., CRGCN, BCIPM). It takes the backbone's learned embeddings as input. Specifically, we denote

$\mathbf{e}_{u,k}, \mathbf{e}_{i,k} \in \mathbb{R}^d$ as the behavior-specific embeddings for user u and item i under behavior k . These embeddings capture user preferences and item attributes at different behavioral stages.

Problem Formulation. The core challenge is multi-behavior bias, a confounder obscuring true preferences. This bias arises from two sources: (1) unique user interaction habits, where users exhibit distinct patterns, and (2) varying item behavior distributions, where items attract different engagement types. These biases create spurious correlations. Our goal is to disentangle the true preference signal from this confounding noise. Formally:

- **Input:** The interaction graphs \mathcal{G} , the multi-behavior bias sets $\{\mathbf{b}_{u,k}, \mathbf{b}_{i,k}\}$, and the backbone embeddings $\{\mathbf{e}_{u,k}, \mathbf{e}_{i,k}\}$.
- **Objective:** Learn an enhancement function $f(\cdot)$ that performs causal debiasing and information fusion to accurately predict the score \hat{y}_{ui} for the target behavior K_t :

$$\hat{y}_{ui} = f(u, i, \{\mathbf{e}_{u,k}, \mathbf{e}_{i,k}\}_{k=1}^K). \quad (1)$$

4 Methodology

In this paper, we propose **MCLMR**, a model-agnostic framework designed to enhance the performance of any backbone multi-behavior recommendation model. The architecture consists of three main modules: **Causal Preference Estimation** for debiased representations, **Adaptive Aggregation** for fusing cross-behavior signals, and **Bias-aware Contrastive Learning** for aligning representations. These modules constitute the training process, while the final prediction relies on a simple inner product in Section 4.4.

4.1 Causal Preference Estimation

To elicit true, unbiased user preferences from data fraught with noise and inherent biases, we adopt a causal inference perspective to disentangle spurious correlations by explicitly modeling the data.

4.1.1 Causal View of Multi-behavior Bias. We construct a causal graph (Figure 2) to identify potential confounders. To facilitate this analysis, we formally define the variables and causal dependencies represented in the graph as follows:

- **U, I:** Feature vectors for users and items, respectively.
- **M (Mediating Behavior):** The initial interaction, determined by feature matching ($\{U, I\}$) and inherent biases (user preference B_u , item tendency B_i).
- **Y (Behavior Outcome):** The final occurrence probability. Our goal is to predict the target outcome Y_{K_t} of the behavior K_t .
- **$\mathbf{B}_u, \mathbf{B}_i$:** Represent the user’s and item’s inherent multi-behavior biases, acting as hidden confounding variables.

The causal relationships identify B_u and B_i as confounders that create backdoor paths (e.g., $U \leftarrow B_u \rightarrow M \rightarrow Y$). Our objective is to block these paths via causal intervention.

Causal Effect Derivation. To estimate the true causal effect, we apply the backdoor adjustment formula based on Pearl’s do-calculus [22]. The interventional probability $P(Y | \text{do}(I), \text{do}(U))$ is given by:

$$P(Y | \text{do}(I), \text{do}(U)) = \sum_{B_i} P(B_i) \sum_{B_u} P(B_u) \times \sum_m P(Y | M = m, I, U) P(M = m | B_i, B_u, I, U). \quad (2)$$

Detailed derivation of Eq. 14 is provided in the appendix A.

4.1.2 Parameterizing Model Components and Biases. To make Eq. 14 tractable, we parameterize the key components, including the multi-behavior biases and the associated probability distributions, and map them to the actual computations within our neural network.

Bias Proxies via Generalized Behavioral Conversion Rate. Using absolute counts can be misleading. To capture intrinsic propensities, we define bias proxies as relative frequencies. The User multi-behavior Bias ($b_{u,k}$) and Item multi-behavior Bias ($b_{i,k}$) are:

$$b_{u,k} = \frac{|\mathcal{I}_u^k|}{\sum_{j=1}^K |\mathcal{I}_u^j|}, \quad b_{i,k} = \frac{|\mathcal{U}_i^k|}{\sum_{j=1}^K |\mathcal{U}_i^j|}. \quad (3)$$

While identifying an optimal proxy for latent confounders remains a widespread challenge in causal debiasing, our approach follows established conventions in the field (e.g., DecRS, iDCF, PDA). We utilize relative frequency as a practical and effective approximation to capture behavioral propensities, though we acknowledge that exploring more complex proxy formulations remains a valuable direction for future work.

Rather than treating these values as simple heuristics, we interpret them as computable proxies for the confounding variables (B_u, B_i) that govern interaction choices. Specifically, $b_{u,k}$ reflects a user’s causal baseline propensity to ‘convert’ a general state of engagement into behavior k . Unlike traditional conversion rates that model pairwise sequential transitions (e.g., view-to-click) with $O(K^2)$ complexity, our *holistic conversion* approach efficiently captures global behavioral tendencies. This formulation provides a rigorous basis for causal adjustment while maintaining efficiency.

Parameterizing Probability Distributions. We approximate the probability terms in the backdoor adjustment (Eq. 14) using the defined components. The initial interaction propensity $P(M_k = 1 | \cdot)$ is modeled as a debiased base score $S_{\text{base},k}$, combining the true matching degree $f_k(u, i)$ and the bias effect $g_k(b_{u,k}, b_{i,k})$:

$$P(M_k = 1 | B_{i,k}, B_{u,k}, U, I) \approx S_{\text{base},k}(u, i) = f_k(u, i) \cdot g_k(b_{u,k}, b_{i,k}). \quad (4)$$

Subsequently, the outcome probability $P(Y_j = 1 | M_k = 1, \dots)$ describes the likelihood of a final behavior j occurring given the initial interaction. This is modulated by auxiliary behaviors via a cross-behavior contribution factor S_{contrib} :

$$P(Y_j = 1 | M_k = 1, u, i) \approx f_j(u, i) \cdot S_{\text{contrib}}(M_k \rightarrow Y_j)(u, i). \quad (5)$$

These parameterizations enable the model to approximate the interventional objective in a computationally tractable manner, laying the foundation for behavior-aware predictions.

4.2 Adaptive Aggregation module

The aggregation mechanism described below is a general framework applicable to any behavior k . For clarity and alignment with our main goal, we illustrate the aggregation mechanism for the target behavior K_t . The training prediction score, $S_{\text{final},K_t}(u, i)$, combines the base score with contributions from auxiliary behaviors:

$$S_{\text{final},K_t}(u, i) = S_{\text{base},K_t}(u, i) \cdot (1 + C_{K_t}(u, i, b_{u,k}, b_{i,k})). \quad (6)$$

Here, the term 1 represents the self-contribution from K_t , while the summation aggregates influence from auxiliary behaviors.

$$C_{K_t}(u, i, b_u, b_i) = \sum_{k \neq K_t} \text{Con}(k \rightarrow K_t)(u, i, b_{u,k}, b_{i,k}). \quad (7)$$

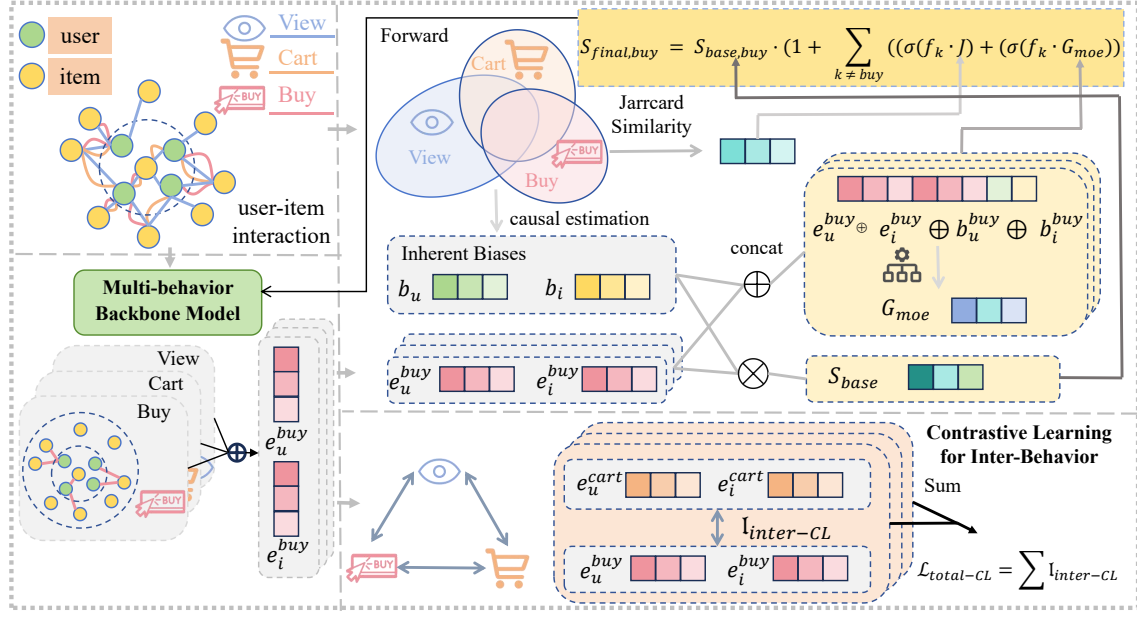


Figure 1: The overall framework of the MCLMR model

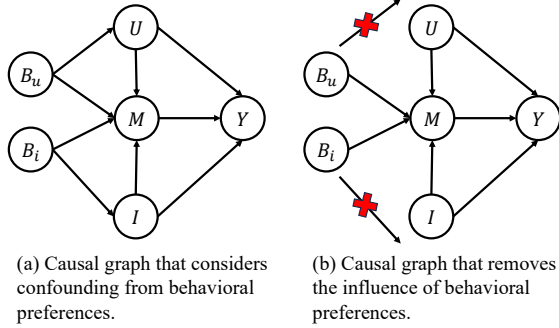


Figure 2: The proposed causal graph to illustrate the relationships among behavioral bias, true user preference, and observed interactions.

Adaptive Aggregation for Training Objective. The contribution $\text{Con}(k \rightarrow K_t)$ is derived from the auxiliary matching degree $f_k(u, i)$, which is dynamically modulated by structural and semantic relevance via a dual-path gating mechanism:

$$\text{Con}(k \rightarrow K_t)(u, i, b_{u,k}, b_{i,k}) = \lambda_J \cdot \sigma(f_k(u, i) \cdot J(u, k, K_t)) + \lambda_M \cdot \sigma(f_k(u, i) \cdot g_{moe}(u, i, k, b_{u,k}, b_{i,k})).$$

where λ_J and λ_M are learnable parameters that balance the influence of the two paths. Next, we detail the estimation of the components in each path.

Structural Gating with Jaccard Similarity. This path's contribution relies on two elements: the true matching degree of the auxiliary behavior, $f_k(u, i)$, and its structural similarity to the target,

$J(u, k, K_t)$. The Jaccard similarity quantifies the overlap of items the user u interacted with under behavior k and K_t .

$$J(u, k, K_t) = \frac{|I_u^k \cap I_u^{K_t}|}{|I_u^k \cup I_u^{K_t}| + \epsilon}. \quad (8)$$

Here, I_u^k denotes the set of items with which user u has interacted under behavior k . By multiplying f_k with this structural score, we ensure that an auxiliary behavior contributes more significantly only if it is both intrinsically preferred and structurally relevant to the target.

Semantic Gating with Mixture-of-Experts (MoE). This path's contribution is also weighted by a semantic relevance score, $g_{moe}(u, i, k)$, from a MoE gating network. The gate dynamically assesses an auxiliary behavior's relevance by processing its corresponding user embeddings, item embeddings, and biases as input.

$$\text{input}_{\text{gate}} = [\mathbf{e}_{u,k}, \mathbf{e}_{i,k}, \mathbf{b}_{u,k}, \mathbf{b}_{i,k}], \quad g_{moe}(u, i, k, b_{u,k}, b_{i,k}) = G_{moe}(\text{input}_{\text{gate}}). \quad (9)$$

This design leverages an MoE gate to assess the semantic value of an auxiliary interaction; it uses the embeddings and biases of a specific behavior, k , to determine if the interaction is a strong signal or noise, thereby uncovering its deep, latent dependencies.

4.3 Bias-aware Contrastive Learning module

To bridge the semantic gaps between behavior-specific representations, we introduce an adaptive contrastive learning framework. This module aligns the representation spaces across different actions, creating a more holistic and consistent user/item profile. Crucially, it mitigates data sparsity in key downstream behaviors

(e.g., purchase) by transferring knowledge from denser, upstream interactions (e.g., view).

4.3.1 Constructing User and Item-centric Contrastive Views. We establish relational alignment from both user and item perspectives, treating each behavior type k as an independent “view”.

For any user u , their embeddings from two different behavioral views (e.g., $\mathbf{e}_u^{\text{view}}$, $\mathbf{e}_u^{\text{purchase}}$) are considered semantically linked and form a Positive Pair. Conversely, embeddings from different users within the same batch (e.g., $\mathbf{e}_u^{\text{view}}$, $\mathbf{e}_v^{\text{purchase}}$) are considered unrelated and form Negative Pairs.

Symmetrically, for any item i , its embeddings from two different behavioral views (e.g., $\mathbf{e}_i^{\text{view}}$, $\mathbf{e}_i^{\text{purchase}}$) constitute a Positive Pair. Embeddings from different items (e.g., $\mathbf{e}_i^{\text{view}}$, $\mathbf{e}_j^{\text{purchase}}$) form Negative Pairs. This encourages the model to learn behavior-invariant item characteristics.

4.3.2 Adaptive Contrastive Objective with Personalized Bias-aware Temperature. We adopt InfoNCE as the contrastive objective. Unlike fixed parameters that ignore heterogeneity, we introduce a personalized *Bias-aware* adaptive temperature. The core intuition is that strong behavioral patterns (e.g., frequent purchases) yield reliable signals, warranting a lower τ to enforce stricter alignment. Conversely, sparse or noisy interactions require a higher τ to prevent overfitting.

Leveraging the cascading nature of multi-behavior data (e.g., view \rightarrow purchase), we define reliability based on the *downstream* behavior’s bias. Consequently, the temperature τ for aligning views $k_i \rightarrow k_j$ is dynamically computed for each user u as:

$$\tau_{u,k_j} = \tau_0 \cdot (1 - \alpha \cdot b_{u,k_j}). \quad (10)$$

where τ_0 is a base temperature, b_{u,k_j} is the user’s bias for the downstream behavior k_j , and $\alpha \in [0, 1)$ is a scaling factor that controls the sensitivity of τ to the bias. An analogous formula is used for item-centric temperature τ_{i,k_j} using item bias b_{i,k_j} .

The final contrastive loss integrates both user and item-centric objectives. The loss for a user u between views k_i and k_j is:

$$\mathcal{L}_{CL-U}(u_{k_i}, u_{k_j}) = -\log \frac{\exp(\text{sim}(\mathbf{e}_u^{k_i}, \mathbf{e}_u^{k_j})/\tau_{u,k_j})}{\sum_{v \in \mathcal{U}} \exp(\text{sim}(\mathbf{e}_u^{k_i}, \mathbf{e}_v^{k_j})/\tau_{u,k_j})}. \quad (11)$$

The total contrastive loss \mathcal{L}_{CL} is the sum of all user-centric and item-centric losses over all pairs of distinct behaviors, balanced by a hyperparameter β :

$$\mathcal{L}_{CL} = \sum_{u, i \neq j} \mathcal{L}_{CL-U}(u_{k_i}, u_{k_j}) + \beta \sum_{i, i' \neq j'} \mathcal{L}_{CL-I}(i_{k_i}, i_{k_j'}). \quad (12)$$

By jointly optimizing this adaptive auxiliary loss, the model learns more robust, coherent, and representations that respect the varying reliability of interaction signals.

4.4 Final Prediction for Recommendation

At the inference stage, the final prediction score \hat{y}_{ui} for the target behavior K_t is determined by the simple inner product of the learned user and item embeddings:

$$\hat{y}_{ui} = \mathbf{e}_{u, K_t} \cdot \mathbf{e}_{i, K_t}^T \quad (13)$$

Table 1: Statistics of the experimental datasets.

Dataset	Users	Items	view	collect	cart	buy
Tmall	41,738	11,953	1,813,498	221,514	1,996	255,586
Jdata	93,334	24,624	1,681,430	45,613	49,891	333,383
Taobao	15,449	11,953	873,954	-	195,476	92,180

This score serves as an unbiased estimate of the true user preference, as confounding biases were addressed during the model’s causal training phase. It is then used to rank items for recommendation.

5 Experiments

In this section, we conduct comprehensive experiments to evaluate MCLMR’s effectiveness, examining its performance improvements across different models and datasets (RQ1), the impact of key components (RQ2), hyperparameter sensitivity (RQ3), the effectiveness of causal deconfounding (RQ4), and computational efficiency (RQ5).

5.1 Experimental Settings

5.1.1 Datasets. We evaluate our proposed method on three real-world public benchmark datasets. The pre-processing of these datasets is consistent with the previous methods [4, 43]. The statistics of these datasets are summarized in Table 1.

5.1.2 Baselines. To validate the effectiveness of MCLMR, we compared it with numerous baseline models in recent years, which can be divided into three categories: (1) Single-behavior methods: MF-BPR [23], NCF [11] and LightGCN [10], (2) Multi-behavior methods: RGCN [24], NMTR [8], MBGCN [13], GNMR [35], S-MBRec [9], MB-HGCN [41], CRGCN [40], BCIPM [42], HEC-GCN [43]. (3) Integrated Causal Multi-behavior methods: CVID [7], CMSR [18]. (4) Pluggable Causal methods: SNIPS [26], Cause [2], Multi-IPW [45], DCCL [47]. We denote the models enhanced by our framework as **LightGCN+MCLMR**, **HEC-GCN+MCLMR**, **CRGCN+MCLMR**, and **BCIPM+MCLMR**.

5.1.3 Evaluation Metrics. To evaluate the performance of top-N recommendation, we adopt two widely used metrics: Hit Ratio (HR@K) and Normalized Discounted Cumulative Gain (NDCG@K). We set K to 10 and 50. The final prediction is made on the target behavior (‘buy’).

5.1.4 Implementation Details. We implement all models in PyTorch on an NVIDIA RTX 4090 GPU using the Adam [14] optimizer. For fair comparison, we adopt optimal backbone settings and fix the embedding size at 64. All MCLMR-specific hyperparameters were carefully tuned; detailed search spaces and final configurations are provided in Appendix B.

5.2 Overall Performance Comparison (RQ1)

To answer RQ1, tables 2 and 3 summarize the comparison results. MCLMR consistently enhances a wide range of backbone models across all datasets, from single-behavior methods to advanced architectures. Notably, the enhancement enables simpler models to surpass complex baselines; for example, LightGCN+MCLMR outperforms CRGCN on Jdata in terms of NDCG@10 (0.2914 vs.

Table 2: Performance Comparison with Various Methods (The best performance is highlighted in bold). The statistical significance of improvements over the best baseline is determined by a paired t-test. Symbols *, **, and * denote statistical significance at the level of $p < 0.05$, $p < 0.01$, and $p < 0.001$, respectively.**

Type	Model	Tmall				Jdata				Taobao			
		H@10	N@10	H@50	N@50	H@10	N@10	H@50	N@50	H@10	N@10	H@50	N@50
Single-behavior Baselines	MF-BPR	0.0230	0.0124	0.0434	0.0166	0.1850	0.1238	0.2652	0.1417	0.0076	0.0036	0.0151	0.0052
	NCF	0.0301	0.0153	0.0678	0.0231	0.2090	0.1410	0.2934	0.1599	0.0236	0.0128	0.0483	0.0175
	LightGCN	0.0463	0.0226	0.1369	0.0414	0.2932	0.1697	0.5374	0.2246	0.0156	0.0077	0.0483	0.0147
	LightGCN+MCLMR	0.1142	0.0583	0.2729	0.0920	0.5026	0.2914	0.7537	0.3503	0.1142	0.0598	0.2815	0.0962
Multi-behavior Baselines	RGCN	0.0316	0.0157	0.0826	0.0262	0.2406	0.1444	0.4873	0.1891	0.0215	0.0104	0.0439	0.0141
	NMTR	0.0517	0.0250	0.1498	0.0456	0.3142	0.1717	0.5227	0.2198	0.0282	0.0137	0.0578	0.0193
	MBGCN	0.0549	0.0285	0.1285	0.0438	0.2803	0.1572	0.5045	0.1984	0.0509	0.0294	0.1009	0.0415
	GNMR	0.0393	0.0193	0.1071	0.0332	0.3068	0.1581	0.4607	0.2029	0.0368	0.0216	0.0735	0.0306
	S-MBRec	0.0694	0.0362	0.1553	0.0544	0.4125	0.2779	0.6036	0.3203	0.1185	0.0659	0.2405	0.0901
	MB-HGCN	0.1461	0.0770	0.3149	0.1130	0.5338	0.3238	0.7749	0.3804	0.1380	0.0728	0.2751	0.1025
	NSED	0.1480	0.0817	0.2814	0.1102	0.5519	0.3378	0.7392	0.3820	0.1652	0.0912	0.2957	0.1198
Integrated Causal Multi-behavior	CVID	0.1542	0.0829	0.3236	0.1215	0.4258	0.2424	0.6685	0.2979	0.1424	0.0768	0.2862	0.1087
	CMSR	0.1585	0.0877	0.3089	0.1206	0.5117	0.3095	0.7276	0.3713	0.1295	0.0713	0.2634	0.0989
Multi-behavior + MCLMR	CRGCN	0.0840	0.0442	0.1994	0.0685	0.4234	0.2479	0.6749	0.3064	0.0882	0.0496	0.1962	0.0730
	CRGCN+MCLMR	0.1449***	0.0803***	0.2725**	0.1075***	0.5003***	0.3054**	0.7007***	0.3521***	0.1464**	0.0839***	0.2753***	0.1122***
	BCIPM	0.1411	0.0741	0.3057	0.1093	0.3851	0.2158	0.6264	0.2711	0.1093	0.0596	0.2462	0.0894
	BCIPM+MCLMR	0.1755	0.0970	0.3320	0.1306	0.5575	0.3381	0.7655	0.3875	0.1635	0.0926	0.3023	0.1232
	HEC-GCN	0.1670	0.0912	0.3131	0.1226	0.5463	0.3360	0.7426	0.3826	0.1807	0.0980	0.3439	0.1341
	HEC-GCN+MCLMR	0.1896**	0.1041**	0.3400**	0.1367**	0.5744***	0.3548**	0.7622***	0.3996***	0.1912**	0.1055***	0.3575*	0.1379*

Table 3: Performance Comparison with Pluggable Causal Models (The best results for each backbone are in bold).

Base Model	Method	Tmall				Jdata				Taobao			
		H@10	N@10	H@50	N@50	H@10	N@10	H@50	N@50	H@10	N@10	H@50	N@50
LightGCN	Original	0.0463	0.0226	0.1369	0.0414	0.2932	0.1697	0.5374	0.2246	0.0156	0.0077	0.0483	0.0147
	+ SNIPS	0.0478	0.0284	0.1533	0.0556	0.4149	0.2438	0.6948	0.3067	0.0141	0.0073	0.0427	0.0134
	+ CausE	0.0390	0.0188	0.1184	0.0351	0.3005	0.1766	0.5654	0.2350	0.0185	0.0089	0.0528	0.0161
	+ Multi-IPW	0.0573	0.0322	0.1738	0.0657	0.4150	0.2520	0.6661	0.3084	0.0241	0.0136	0.0745	0.0241
	+ DCCL	0.0952	0.0497	0.2386	0.0799	0.4822	0.2886	0.7347	0.3472	0.1067	0.0553	0.2629	0.0890
	+ MCLMR	0.1142	0.0583	0.2729	0.0920	0.5026	0.2914	0.7537	0.3503	0.1142	0.0598	0.2815	0.0962
CRGCN	Original	0.0840	0.0442	0.1994	0.0685	0.4234	0.2479	0.6749	0.3064	0.0882	0.0496	0.1962	0.0730
	+ SNIPS	0.1197	0.0654	0.2615	0.0955	0.4283	0.2456	0.6788	0.3041	0.1082	0.0635	0.2205	0.0879
	+ CausE	0.1185	0.0632	0.2608	0.0933	0.3828	0.2161	0.6299	0.2727	0.0917	0.0518	0.1998	0.0752
	+ Multi-IPW	0.1201	0.0654	0.2590	0.0950	0.4189	0.2432	0.6722	0.3024	0.1080	0.0633	0.2207	0.0878
	+ DCCL	0.1144	0.0624	0.2381	0.0886	0.4699	0.2860	0.6833	0.3353	0.1174	0.0667	0.2432	0.0942
	+ MCLMR	0.1449	0.0803	0.2725	0.1075	0.5003	0.3054	0.7007	0.3521	0.1464	0.0839	0.2753	0.1122
HEC-GCN	Original	0.1670	0.0912	0.3131	0.1226	0.5463	0.3360	0.7426	0.3826	0.1807	0.0980	0.3439	0.1341
	+ SNIPS	0.1744	0.0950	0.3278	0.1279	0.5156	0.3148	0.7080	0.3597	0.1851	0.1027	0.3345	0.1358
	+ CausE	0.1768	0.0961	0.3365	0.1308	0.5568	0.3396	0.7459	0.3842	0.1847	0.1005	0.3340	0.1334
	+ Multi-IPW	0.1523	0.0824	0.3047	0.115	0.5275	0.3167	0.7548	0.3701	0.1584	0.0862	0.3312	0.1241
	+ DCCL	0.1759	0.0967	0.3237	0.1286	0.5346	0.3250	0.7306	0.3711	0.1863	0.1034	0.3259	0.1342
	+ MCLMR	0.1896	0.1041	0.3400	0.1367	0.5744	0.3548	0.7622	0.3996	0.1912	0.1055	0.3575	0.1379

0.2479). Substantial improvements are also observed in strong, specialized models (e.g., HEC-GCN on Tmall). Furthermore, compared with other pluggable causal methods like SNIPS and DCCL, our framework achieves superior performance on identical backbones, validating its effectiveness and model-agnostic nature.

5.3 Ablation Study (RQ2)

To answer RQ2, We conduct a comprehensive ablation study using CRGCN and BCIPM on Tmall and Jdata to validate MCLMR’s components. We compare the full model against six variants: (1) **w/o U-Bias**: Removes the debiasing module for user behavior habits. (2) **w/o I-Bias**: Removes the debiasing module for item multi-behavior

bias. (3) **w/o Agg.**: Removes the entire adaptive information aggregation module. (4) **w/o Jaccard**: Removes the Jaccard gate within the aggregation module. (5) **w/o MoE**: Removes the Mixture-of-Experts (MoE) gate within the aggregation module. (6) **w/o CL**: Removes the contrastive learning module.

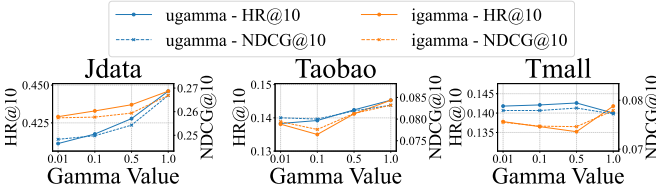
As detailed in Tables 4 and 5, the full model consistently yields the best performance. The degradation across all variants confirms that every component is indispensable. Specifically, the significant drop in **w/o CL** identifies contrastive learning as a critical regularizer. Similarly, declines in **w/o Agg.** and **w/o U/I-Bias** validate the vital roles of adaptive aggregation in preventing negative transfer and causal debiasing in disentangling confounders.

Table 4: Ablation study results on the Tmall dataset. The best performance for each backbone is in bold.

Model Variant	BCIPM+MCLMR		CRGCN+MCLMR	
	HR@10	NDCG@10	HR@10	NDCG@10
w/o U-Bias	0.1724	0.0949	0.1385	0.0763
w/o I-Bias	0.1716	0.0932	0.1380	0.0756
w/o Jaccard	0.1737	0.0946	0.1323	0.0718
w/o MoE	0.1719	0.0945	0.1400	0.0771
w/o Agg.	0.1675	0.0925	0.1309	0.0705
w/o CL	0.1476	0.0805	0.1213	0.0557
Full Model	0.1755	0.0970	0.1449	0.0803

Table 5: Ablation study results on the Jdata dataset. The best performance for each backbone is in bold.

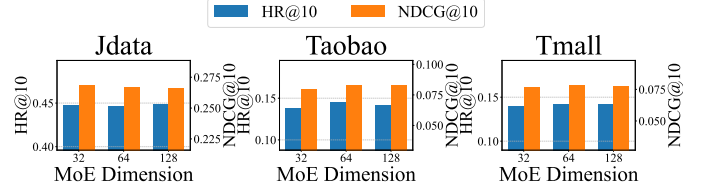
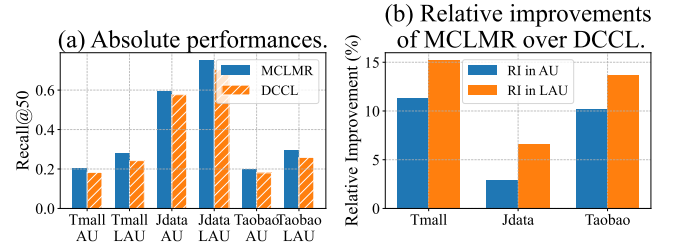
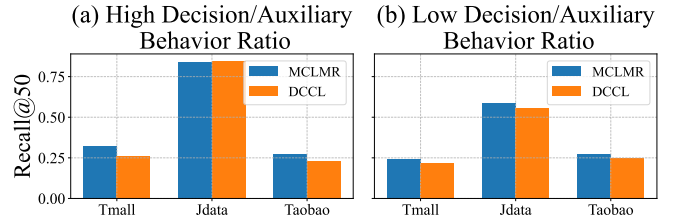
Model Variant	BCIPM+MCLMR		CRGCN+MCLMR	
	HR@10	NDCG@10	HR@10	NDCG@10
w/o U-Bias	0.5431	0.3301	0.4518	0.2741
w/o I-Bias	0.5454	0.3320	0.4623	0.2797
w/o Jaccard	0.5539	0.3359	0.4694	0.2843
w/o MoE	0.5542	0.3361	0.4709	0.2865
w/o Agg.	0.5461	0.3328	0.4597	0.2770
w/o CL	0.4521	0.2660	0.4567	0.2522
Full Model	0.5575	0.3381	0.5003	0.3054

**Figure 3: Impact of the debiasing coefficient γ . Performance is shown for HR@10 (left) and NDCG@10 (right).**

5.4 Parameter Analysis (RQ3)

This subsection examines MCLMR’s sensitivity to hyperparameters using the CRGCN backbone. Regarding the debiasing coefficient γ (Fig. 3), a small value (0.01) is universally optimal for items, whereas the optimal user γ is dataset-dependent (larger for Jdata, smaller for Taobao). For the MoE expert dimension (Fig. 4), performance peaks at 64, providing the optimal trade-off between expressiveness and generalization; larger capacities lead to overfitting.

Effectiveness of Bias-aware Temperature. We investigate the temperature parameter τ in our contrastive loss. Unlike standard fixed or learnable approaches, we dynamically adapt τ to behavioral biases to balance the primary BPR and auxiliary contrastive tasks. Specifically, high-bias behaviors (dominating BPR) require distinct penalties compared to sparse ones. We validate this design against four variants (Fixed, Learnable, Random, Alternative Mappings), with detailed settings and comparisons provided in Appendix C.

**Figure 4: Impact of the MoE expert dimension. Performance is shown for HR@10 (left) and NDCG@10 (right).****Figure 5: Performance of CRGCN+MCLMR and CRGCN+DCCL in active and less-active user groups. (a) the absolute performance; and (b) the relative improvements of MCLMR over DCCL. "AU" and "LAU" are short for the active user group and the less-active user group, respectively. In (a), bars with slash and without slash corresponds to DCCL and MCLMR, respectively. Better viewed in color.****Figure 6: Recall@50 of CRGCN+MCLMR and CRGCN+DCCL in item groups with high and low Decision/Auxiliary Behavior ratio.**

5.5 In-depth Analyses (RQ4)

In this subsection, we conduct a detailed analysis using the CRGCN backbone to investigate three key questions (analyses on other backbones like HECGCN and LightGCN are deferred to Appendix D). Specifically, we aim to determine: 1) the primary sources of performance improvements; 2) consistency across different user groups; and 3) effectiveness in recommending high-quality items.

5.5.1 Improvements in Active and Less-active User Groups. We examine whether MCLMR benefits active or less-active user groups differently. For Tmall, Jdata, and Taobao, the top 20% of users by

interaction count are classified as *active* (AU), and the rest as *less-active* (LAU). We compare MCLMR and DCCL on: 1) absolute Recall@50 performance; and 2) relative improvements.

Figure 5 summarizes the results. We observe that: 1) Better Performance in LAU: As shown in Fig. 5(a), both models perform better in the LAU group across all datasets. 2) Overall Superiority: MCLMR consistently outperforms DCCL in both active and less-active groups. 3) Greater Relative Improvement in LAU: As shown in Fig. 5(b), the relative improvement (RI) of MCLMR over DCCL is notably higher in the LAU group. These results indicate MCLMR is particularly effective for long-tail users, helping alleviate the ‘‘Matthew effect’’ by ensuring less-active users receive high-quality recommendations despite sparse histories.

5.5.2 Recommendation Quality w.r.t. Decision/Auxiliary Behavior Ratio. Whether the proposed MCLMR can achieve consistent and unbiased user preference estimations is our concern. Thus, in this part, we sort items according to the *decision/auxiliary behavior ratio* and divide them into two groups: the top 20% of items with a high ratio, and the remaining 80% with a low ratio. High-ratio items are considered higher quality as they align with target actions, whereas over-recommending low-ratio items may hurt user experience. We use recall for evaluation.

The performance on these groups is shown in Figure 6. In the high-ratio group (Figure 6(a)), MCLMR significantly outperforms DCCL on Tmall and Taobao, with comparable results on Jdata, demonstrating its capability to recommend high-quality items. Furthermore, in the low-ratio group (Figure 6(b)), MCLMR consistently leads across all datasets. These results suggest that MCLMR is more precise in recommending high-quality items and robust in handling low-quality ones. We attribute this to the removal of hidden confounders that might otherwise promote items with high auxiliary engagement but low decision value.

5.6 Complexity Analysis (RQ5)

To evaluate the computational overhead of our proposed MCLMR framework, we analyze its time complexity in comparison with three state-of-the-art multi-behavior recommendation models: CRGCN, HEC-GCN, and BCIPM.

5.6.1 Notations. We define the following symbols: U and I are the total number of users and items; d is the embedding dimension; B is the number of behaviors; K is the number of GCN layers; E_{total} is the total number of edges across all behaviors; H is the number of hyperedges in the hypergraph; and u_s is the number of unique users within a batch.

5.6.2 Complexity of the MCLMR Framework. Our MCLMR framework introduces an additional computational overhead, O_{MCLMR} , which is composed of three main modules: (1) Jaccard Aggregation Module: $O(N \cdot B^2 \cdot r)$. (2) MoE Gating Aggregation Module: $O(N \cdot B^2 \cdot k \cdot d)$. (3) Multi-behavior Contrastive Learning Module: $O((u_s + i_s) \cdot B^2 \cdot d^2)$. Thus, the total incremental complexity is $O_{\text{MCLMR}} = O(N \cdot B^2 \cdot (r + k \cdot d) + (u_s + i_s) \cdot B^2 \cdot d^2)$.

5.6.3 Complexity Comparison and Analysis. Table 6 summarizes the original dominant complexities of the backbone models and the total complexity after integrating MCLMR.

Table 6: Time complexity of baseline models before and after integration with the MCLMR framework.

Model	Core Computational Modules	Dominant Time Complexity
HEC-GCN	GCNs & Hypergraph GCN & Attention & Contrastive Learning	$O(L \cdot E_{\text{total}} \cdot d + K \cdot (M + N) \cdot S \cdot d + K \cdot (M^2 + N^2) \cdot d)$
CRGCN	Cascading GCN Propagation	$O(K \cdot E_{\text{total}} \cdot d)$
BCIPM	GCNs & Neighborhood Aggregation	$O(K \cdot E_{\text{total}} \cdot d + b_s \cdot L_{\text{max}} \cdot d^2)$
+MCLMR	+ Adaptive Aggregation + Bias-aware CL	$+O(N \cdot B^2 \cdot (r + k \cdot d) + (u_s + i_s) \cdot B^2 \cdot d^2)$

The analysis confirms that MCLMR introduces a fixed computational overhead, demonstrating its model-agnostic nature. The relative impact of this overhead is more significant on simpler models like CRGCN but less pronounced on inherently complex ones such as HEC-GCN. Notably, for BCIPM, our framework adds a complexity term that scales with the square of the batch size (u_s^2), increasing the model’s sensitivity to this hyperparameter.

Empirical Runtime and Latency. In addition to the theoretical complexity analysis, we evaluated the actual training overhead and online inference latency on real-world GPUs to demonstrate its practical efficiency. The empirical results confirm that MCLMR introduces only a minor increase in training time (e.g., approx. 4% increase for HEC-GCN) while maintaining the same inference speed as the backbone models. A detailed derivation of the theoretical complexities can be found in **Appendix E**, and the comprehensive empirical runtime statistics are provided in **Appendix F**.

5.7 Ethical Considerations

We acknowledge the importance of ethical data usage in recommender systems. This work utilizes public, anonymized datasets (Tmall, Jdata, Taobao) to strictly protect user privacy. Furthermore, our proposed causal debiasing framework is explicitly designed to mitigate behavioral biases, contributing to more fair and unbiased recommendation outcomes.

6 Conclusion

In this paper, we propose MCLMR, a novel model-agnostic causal learning framework that addresses multi-behavior biases in recommendation systems. We first construct a causal graph to model the complex confounding effects from user behavioral habits and item multi-behavior distributions. Then we design an Adaptive Aggregation module based on Mixture-of-Experts to dynamically fuse auxiliary behaviors, and a Bias-aware Contrastive Learning module with user-item dual alignment to bridge semantic gaps while accounting for bias distortions. Extensive experiments on three real-world datasets demonstrate that MCLMR consistently improves various existing MBR models, validating its effectiveness.

Acknowledgments

This work was supported in part by the Natural Science Foundation of Anhui Province (Grant No. 2508085QF211), the National Natural Science Foundation of China (Grant No. 62506348), New Generation Artificial Intelligence-National Science and Technology Major Project (Grant No. 2025ZD0122601), the Opening Foundation of State Key Laboratory of Cognitive Intelligence, iFLYTEK (COGOS-2025HE02), the CCF-1688 Yuanbao Cooperation Fund (Grant No. CCF-Alibaba2025005).

References

- [1] Himan Abdollahpouri and Masoud Mansoury. 2020. Multi-sided Exposure Bias in Recommendation. *arXiv e-prints*, Article arXiv:2006.15772 (June 2020), arXiv:2006.15772 pages. arXiv:2006.15772 [cs.LG] doi:10.48550/arXiv.2006.15772
- [2] Stephen Bonner and Flavian Vasile. 2018. Causal embeddings for recommendation. In *Proceedings of the 12th ACM Conference on Recommender Systems* (Vancouver, British Columbia, Canada) (*RecSys '18*). Association for Computing Machinery, New York, NY, USA, 104–112. doi:10.1145/3240323.3240360
- [3] Léon Bottou, Jonas Peters, Joaquin Quiñero Candela, Denis X. Charles, D. Max Chickering, Elon Portugaly, Dipankar Ray, Patrice Simard, and Ed Snelson. 2013. Counterfactual reasoning and learning systems: the example of computational advertising. *J. Mach. Learn. Res.* 14, 1 (Jan. 2013), 3207–3260.
- [4] Wei Cai, ZhiHong Zheng, Xuan Zhang, WeiYi Shang, Yubin Ma, WenJie Gao, and Zhi Jin. 2025. Neighborhood structure enhancement and denoising method for multi-behavior recommendation. *Neural Networks* 191 (2025), 107760. doi:10.1016/j.neunet.2025.107760
- [5] Jiawei Chen, Hande Dong, Xiang Wang, Fuli Feng, Meng Wang, and Xiangnan He. 2021. Bias and Debias in Recommender System: A Survey and Future Directions. arXiv:2010.03240 [cs.LG] https://arxiv.org/abs/2010.03240
- [6] Jiawei Chen, Hande Dong, Xiang Wang, Fuli Feng, Meng Wang, and Xiangnan He. 2023. Bias and Debias in Recommender System: A Survey and Future Directions. *ACM Trans. Inf. Syst.* 41, 3, Article 67 (Feb. 2023), 39 pages. doi:10.1145/3564284
- [7] Yuzhe Chen, Jie Cao, Youquan Wang, Jia Wu, Huanhuan Chen, and Guandong Xu. 2025. Causal Variational Inference for Deconfounded Multi-Behavior Recommendation. *ACM Trans. Inf. Syst.* 43, 6, Article 151 (Sept. 2025), 26 pages. doi:10.1145/3745023
- [8] Chen Gao, Xiangnan He, Dahua Gan, Xiangning Chen, Fuli Feng, Yong Li, Tat-Seng Chua, and Depeng Jin. 2019. Neural multi-task recommendation from multi-behavior data. In *ICDE*. IEEE, 1554–1557.
- [9] Shuyun Gu, Xiao Wang, Chuan Shi, and Ding Xiao. 2022. Self-supervised Graph Neural Networks for Multi-behavior Recommendation. In *Proceedings of the Thirty-First International Joint Conference on Artificial Intelligence, IJCAI-22*. 2052–2058.
- [10] Xiangnan He, Kuan Deng, Xiang Wang, Yan Li, Yongdong Zhang, and Meng Wang. 2020. LightGCN: Simplifying and Powering Graph Convolution Network for Recommendation. *arXiv preprint arXiv:2002.02126* (2020).
- [11] Xiangnan He, Lizi Liao, Hanwang Zhang, Liqiang Nie, Xia Hu, and Tat-Seng Chua. 2017. Neural collaborative filtering. In *WWW*. 173–182.
- [12] Chao Huang. 2021. Recent Advances in Heterogeneous Relation Learning for Recommendation. *arXiv preprint arXiv:2110.03455* (2021).
- [13] Bowen Jin, Chen Gao, Xiangnan He, Depeng Jin, and Yong Li. 2020. Multi-behavior recommendation with graph convolutional networks. In *SIGIR*.
- [14] Diederik P Kingma and Jimmy Ba. 2014. Adam: A method for stochastic optimization. *arXiv preprint arXiv:1412.6980* (2014).
- [15] Karl Krauth, Yixin Wang, and Michael I. Jordan. 2022. Breaking Feedback Loops in Recommender Systems with Causal Inference. arXiv:2207.01616 [cs.LG] https://arxiv.org/abs/2207.01616
- [16] Jie Liao, Min Yang, Wei Zhou, Hongyu Zhang, and Junhao Wen. 2024. Modeling item exposure and user satisfaction for debiased recommendation with causal inference. *Inf. Sci.* 676, C (Aug. 2024), 15 pages. doi:10.1016/j.ins.2024.120834
- [17] Lingfeng Liu, Yixin Song, Dazhong Shen, Bing Yin, Hao Li, Yanyong Zhang, and Chao Wang. 2025. Rethinking Popularity Bias in Collaborative Filtering via Analytical Vector Decomposition. *arXiv preprint arXiv:2512.10688* (2025).
- [18] Dan Lu, Shiqing Wu, Hao Zhang, Guandong Xu, and Qilong Han. 2025. Causal cascading convolution networks for multi-behavior sequential recommendation. *Information Sciences* 720 (2025), 122484. doi:10.1016/j.ins.2025.122484
- [19] Huishi Luo, Fuzhen Zhuang, Ruobing Xie, Hengshu Zhu, Deqing Wang, Zhulin An, and Yongjun Xu. 2024. A survey on causal inference for recommendation. *The Innovation* 5, 2 (2024), 100590. doi:10.1016/j.xinn.2024.100590
- [20] Chenglong Ma, Ziqi Xu, Yongli Ren, Danula Hettiaachchi, and Jeffrey Chan. 2025. PUB: An LLM-Enhanced Personality-Driven User Behaviour Simulator for Recommender System Evaluation. In *Proceedings of the 48th International ACM SIGIR Conference on Research and Development in Information Retrieval, SIGIR*. 2690–2694. https://doi.org/10.1145/3726302.3730238
- [21] Masoud Mansoury, Bamshad Mobasher, and Herke van Hoof. 2024. Mitigating Exposure Bias in Online Learning to Rank Recommendation: A Novel Reward Model for Cascading Bandits. In *Proceedings of the 33rd ACM International Conference on Information and Knowledge Management* (Boise, ID, USA) (*CIKM '24*). Association for Computing Machinery, New York, NY, USA, 1638–1648. doi:10.1145/3627673.3679763
- [22] Judea Pearl. 2009. *Causality: Models, Reasoning and Inference* (2nd ed.). Cambridge University Press, USA.
- [23] Steffen Rendle, Christoph Freudenthaler, Zeno Gantner, and Lars Schmidt-Thieme. 2012. BPR: Bayesian personalized ranking from implicit feedback. *arXiv preprint arXiv:1205.2618* (2012).
- [24] Michael Schlichtkrull, Thomas N Kipf, Peter Bloem, Rianne Van Den Berg, Ivan Titov, and Max Welling. 2018. Modeling relational data with graph convolutional networks. In *European semantic web conference*. Springer, 593–607.
- [25] Xiaoyuan Su and Taghi M Khoshgoftaar. 2009. A survey of collaborative filtering techniques. *Advances in artificial intelligence* 2009 (2009).
- [26] Adith Swaminathan and Thorsten Joachims. 2015. The Self-Normalized Estimator for Counterfactual Learning. In *Advances in Neural Information Processing Systems*, C. Cortes, N. Lawrence, D. Lee, M. Sugiyama, and R. Garnett (Eds.), Vol. 28. Curran Associates, Inc. https://proceedings.neurips.cc/paper_files/paper/2015/file/39027dfad5138c9ca0c474d71db915c3-Paper.pdf
- [27] Chao Wang, Qi Liu, Runze Wu, Enhong Chen, Chuanren Liu, Xunpeng Huang, and Zhenya Huang. 2018. Confidence-aware matrix factorization for recommender systems. In *Proceedings of the AAAI Conference on artificial intelligence*, Vol. 32.
- [28] Chao Wang, Yixin Song, Jinhui Ye, Chuan Qin, Dazhong Shen, Lingfeng Liu, Xiang Wang, and Yanyong Zhang. 2025. FACE: A General Framework for Mapping Collaborative Filtering Embeddings into LLM Tokens. *arXiv preprint arXiv:2510.15729* (2025).
- [29] Chao Wang, Hengshu Zhu, Qiming Hao, Keli Xiao, and Hui Xiong. 2021. Variable interval time sequence modeling for career trajectory prediction: Deep collaborative perspective. In *Proceedings of the Web Conference 2021*. 612–623.
- [30] Chao Wang, Hengshu Zhu, Peng Wang, Chen Zhu, Xi Zhang, Enhong Chen, and Hui Xiong. 2021. Personalized and explainable employee training course recommendations: A bayesian variational approach. *ACM Transactions on Information Systems (TOIS)* 40, 4 (2021), 1–32.
- [31] Chao Wang, Hengshu Zhu, Chen Zhu, Chuan Qin, and Hui Xiong. 2020. Setrank: A setwise bayesian approach for collaborative ranking from implicit feedback. In *Proceedings of the aaii conference on artificial intelligence*, Vol. 34. 6127–6136.
- [32] Yixin Wang, Dawen Liang, Laurent Charlin, and David M. Blei. 2018. The Deconfounded Recommender: A Causal Inference Approach to Recommendation. *arXiv e-prints*, Article arXiv:1808.06581 (Aug. 2018), arXiv:1808.06581 pages. arXiv:1808.06581 [cs.LG] doi:10.48550/arXiv.1808.06581
- [33] Xinye Wanyan, Danula Hettiaachchi, Chenglong Ma, Ziqi Xu, and Jeffrey Chan. 2025. Temporal-Aware User Behaviour Simulation with Large Language Models for Recommender Systems. In *Proceedings of the 34th ACM International Conference on Information and Knowledge Management, CIKM*. 5335–5339. https://doi.org/10.1145/3746252.3760878
- [34] Tianxin Wei, Fuli Feng, Jiawei Chen, Ziwei Wu, Jinfeng Yi, and Xiangnan He. 2021. Model-Agnostic Counterfactual Reasoning for Eliminating Popularity Bias in Recommender System. In *Proceedings of the 27th ACM SIGKDD Conference on Knowledge Discovery & Data Mining*. 1791–1800.
- [35] Lianghao Xia, Chao Huang, Yong Xu, Peng Dai, Mengyin Lu, and Liefeng Bo. 2021. Multi-Behavior Enhanced Recommendation with Cross-Interaction Collaborative Relation Modeling. In *ICDE*. IEEE, 1931–1936.
- [36] Lianghao Xia, Chao Huang, Yong Xu, Peng Dai, Bo Zhang, and Liefeng Bo. 2020. Multiplex behavioral relation learning for recommendation via memory augmented transformer network. In *SIGIR*. 2397–2406.
- [37] Ziqi Xu, Debo Cheng, Jiuyong Li, Jixue Liu, Lin Liu, and Ke Wang. 2023. Disentangled Representation for Causal Mediation Analysis. In *Thirty-Seventh AAAI Conference on Artificial Intelligence, AAAI 10666–10674*. https://doi.org/10.1609/aaai.v37i9.26266
- [38] Ziqi Xu, Debo Cheng, Jiuyong Li, Jixue Liu, Lin Liu, and Kui Yu. 2024. Causal Inference with Conditional Front-Door Adjustment and Identifiable Variational Autoencoder. In *The Twelfth International Conference on Learning Representations, ICLR*. https://openreview.net/forum?id=wff9m4v7oC
- [39] Hongrui Xuan, Yi Liu, Bohan Li, and Hongzhi Yin. 2023. Knowledge Enhancement for Contrastive Multi-Behavior Recommendation. In *Proceedings of the Sixteenth ACM International Conference on Web Search and Data Mining*. 195–203.
- [40] Mingshi Yan, Zhiyong Cheng, Chen Gao, Jing Sun, Fan Liu, Fuming Sun, and Haojie Li. 2023. Cascading Residual Graph Convolutional Network for Multi-Behavior Recommendation. 42, 1, Article 10 (Aug. 2023), 26 pages. doi:10.1145/3587693
- [41] Mingshi Yan, Zhiyong Cheng, Jing Sun, Fuming Sun, and Yuxin Peng. 2023. MB-HGCN: A hierarchical graph convolutional network for multi-behavior recommendation. *arXiv preprint arXiv:2306.10679* (2023).
- [42] Mingshi Yan, Fan Liu, Jing Sun, Fuming Sun, Zhiyong Cheng, and Yahong Han. 2024. Behavior-Contextualized Item Preference Modeling for Multi-Behavior Recommendation. In *Proceedings of the 47th International ACM SIGIR Conference on Research and Development in Information Retrieval*. 946–955.
- [43] Yabo Yin, Xiaofei Zhu, Wenshan Wang, Yihao Zhang, Pengfei Wang, Yixing Fan, and Jiafeng Guo. 2024. HEC-GCN: Hypergraph Enhanced Cascading Graph Convolution Network for Multi-Behavior Recommendation. arXiv:2412.14476 [cs.LG] https://arxiv.org/abs/2412.14476
- [44] Guixian Zhang, Guan Yuan, Debo Cheng, Lin Liu, Jiuyong Li, Ziqi Xu, and Shichao Zhang. 2025. Deconfounding representation learning for mitigating latent confounding effects in recommendation. *Knowledge and Information Systems* 67, 7 (2025), 5999–6020. https://doi.org/10.1007/s10115-025-02404-7
- [45] Wenhao Zhang, Wentian Bao, Xiao-Yang Liu, Keping Yang, Quan Lin, Hong Wen, and Ramin Ramezani. 2019. A Causal Perspective to Unbiased Conversion Rate Estimation on Data Missing Not at Random. *CoRR* abs/1910.09337 (2019). arXiv:1910.09337 http://arxiv.org/abs/1910.09337

- [46] Yang Zhang, Fuli Feng, Xiangnan He, Tianxin Wei, Chonggang Song, Guohui Ling, and Yongdong Zhang. 2021. Causal Intervention for Leveraging Popularity Bias in Recommendation. In *Proceedings of the 44th International ACM SIGIR Conference on Research and Development in Information Retrieval* (Virtual Event, Canada) (*SIGIR '21*). Association for Computing Machinery, New York, NY, USA, 11–20. doi:10.1145/3404835.3462875
- [47] Weiqi Zhao, Dian Tang, Xin Chen, Dawei Lv, Daoli Ou, Biao Li, Peng Jiang, and Kun Gai. 2023. Disentangled Causal Embedding With Contrastive Learning For Recommender System. In *Companion Proceedings of the ACM Web Conference 2023* (Austin, TX, USA) (*WWW '23 Companion*). Association for Computing Machinery, New York, NY, USA, 406–410. doi:10.1145/3543873.3584637
- [48] Zhe Zhao, Zhiyuan Cheng, Lichan Hong, and Ed H Chi. 2015. Improving user topic interest profiles by behavior factorization. In *Proceedings of the 24th International Conference on World Wide Web*. 1406–1416.
- [49] Yunqin Zhu, Chao Wang, Qi Zhang, and Hui Xiong. 2024. Graph signal diffusion model for collaborative filtering. In *Proceedings of the 47th International ACM SIGIR Conference on Research and Development in Information Retrieval*. 1380–1390.

A Causal Effect Derivation

To block the backdoor paths created by confounding biases, we apply causal intervention using Pearl’s do-calculus. We aim to compute the interventional probability $P(Y|do(I), do(U))$, which represents the unbiased user preference. The derivation, based on the intervened graph G_{do} , is as follows:

$$P(Y|do(I), do(U)) = P_{G_{do}}(Y|I, U) \quad (14a)$$

$$= \sum_{m, B_i, B_u} P_{G_{do}}(Y, M = m, B_i, B_u|I, U) \quad (14b)$$

$$= \sum_{m, B_i, B_u} P_{G_{do}}(Y|M, B_i, B_u, I, U) \quad (14c)$$

$$\times P_{G_{do}}(M|B_i, B_u, I, U) \times P_{G_{do}}(B_i|I, U) P_{G_{do}}(B_u|B_i, I, U) \quad (14d)$$

$$= \sum_{m, B_i, B_u} P(Y|M, I, U) P(M|B_i, B_u, I, U) \times P(B_i) P(B_u) \quad (14d)$$

$$= \sum_{B_i} P(B_i) \sum_{B_u} P(B_u) \sum_m P(Y|M = m, I, U) \times P(M = m|B_i, B_u, I, U) \quad (14e)$$

The derivation steps are justified as follows:

- (14a) is based on the definition of the do-operator, which equates an intervention on a variable to conditioning on it in the manipulated graph G_{do} .
- (14b) is due to the law of total probability, marginalizing over the mediator variables M (user’s real-time intention), B_i (item’s bias), and B_u (user’s bias).
- (14c) applies the chain rule of probability to the joint probability distribution within the summation.
- (14d) is based on the conditional independencies in G_{do} . The interventions $do(I)$ and $do(U)$ block the backdoor paths, making the outcome Y independent of the biases B_i, B_u given $\{M, I, U\}$. Since B_i and B_u are exogenous, they are independent of the interventions. We then apply the mechanism invariance assumption to replace probabilities from G_{do} with those from the observational graph G .
- (14e) is a rearrangement of the terms from the previous step to arrive at the final backdoor adjustment formula, which corresponds to Equation 2 in the main paper.

B Hyperparameter Settings

We conduct a comprehensive grid search for MCLMR’s specific hyperparameters. The key search spaces are:

- **Causal Debiasing** (γ_u, γ_i): The coefficients for user and item multi-behavior biases are searched within $\{0.01, 0.1, 0.5, 1.0\}$.
- **MoE Gate**: The hidden dimension for experts is tuned amongst $\{32, 64, 128\}$.
- **Contrastive Learning**: The temperature τ and weight λ_{CL} are tuned to balance the auxiliary task.

Final configurations for reproducibility are available in the released source code.

C Detailed Analysis of Bias-aware Temperature

This section analyzes the rationale and empirical superiority of our bias-aware temperature mechanism.

C.1 Theoretical Justification

Temperature τ in InfoNCE controls distribution smoothness and hard negative penalties. Our design balances supervised (BPR) and self-supervised (CL) tasks: (1) Redundancy in High-Bias Behaviors: High-bias entities (e.g., active users) dominate BPR gradient updates. To reduce redundancy in the auxiliary task, we assign them a lower temperature to sharpen the distribution. (2) Signal in Low-Bias Behaviors: Sparse behaviors provide weak signals. We assign them a higher temperature (closer to τ_0) to maintain a softer distribution, preventing overfitting to noise offering auxiliary supervision.

C.2 Experimental Variants

We compared our strategy (Eq 10 : $\tau = \tau_0 \cdot (1 - \alpha \cdot b)$) against four variants: (1) Fixed Temperature: τ is set to a constant scalar (e.g., 0.1). (2) Learnable Temperature: τ is a trainable parameter optimized via backpropagation. (3) Random Temperature: τ is sampled from $U(0.1, 0.5)$, inspired by SimGCL. (4) Alternative Mappings: Linear ($\tau = \tau_0(1 + \alpha b)$) and Inverse ($\tau = \tau_0(1 - \alpha/b)$) mappings.

C.3 Performance Comparison

Table 7 shows the performance on the CRGCN backbone.

Table 7: Performance comparison of temperature strategies on CRGCN (HR@50 and NDCG@50).

Method Variant	Jdata		Taobao		Tmall	
	HR@50	NDCG@50	HR@50	NDCG@50	HR@50	NDCG@50
Variant 1: Fixed Temperature	0.7150	0.3414	0.2631	0.1091	0.2650	0.1009
Variant 2: Alt. Mapping ($1 + \alpha \cdot b$)	0.6422	0.3213	0.2623	0.1098	0.2622	0.1035
Variant 3: Learnable Temperature	0.6775	0.3419	0.2481	0.1008	0.2703	0.1044
Variant 4: Random Temperature	0.6970	0.3171	0.2464	0.0990	0.2574	0.0957
MCLMR (Ours)	0.7295	0.3801	0.2736	0.1120	0.2753	0.1075

C.3.1 Analysis. Our bias-aware strategy consistently outperforms all variants (Table 7): (1) vs. Fixed & Random: Random temperature (Var 4) lacks behavioral priors, while Fixed temperature (Var 1) ignores heterogeneity of user activity. (2) vs. Learnable: Directly learning τ (Var 3) underperforms, suggesting without explicit bias-aware guidance, the model fails to optimally balance BPR and CL tasks. (3) vs. Alternatives: The performance drop in Variant 2 confirms that lowering τ for high-bias instances is the correct direction.

These results validate that incorporating a bias-aware prior is crucial for multi-behavior contrastive learning.

D Detailed Analysis with Other Backbones

In this section, we provide supplementary results for our in-depth analysis, using HECGCN and LightGCN as alternative GCN backbones. This complements the primary analysis in the main text, which utilizes CRGCN. The experimental setup for user/item group division and evaluation methodology remains consistent with that described in the main paper.

D.1 Analysis with HECGCN Backbone

We first replace the CRGCN backbone with HECGCN to validate the generalizability of our model’s improvements.

D.1.1 Performance in User Groups. As shown in Figure 7, the results with the HECGCN backbone are consistent with our findings. Our proposed model (HECGCN+MCLMR) consistently outperforms the baseline (HECGCN+DCCL) in both active and less-active user groups. More importantly, the relative improvement is more pronounced in the less-active user group, once again demonstrating our model’s effectiveness in alleviating data sparsity issues.

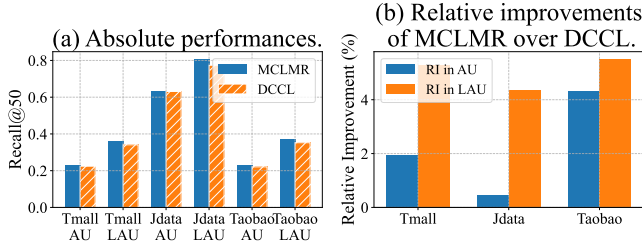


Figure 7: Performance comparison with the HECGCN backbone in active (AU) and less-active (LAU) user groups. (a) Absolute performance; (b) Relative improvements of MCLMR over DCCL.

D.1.2 Recommendation Quality. Figure 8 illustrates the recommendation quality on items with different decision/auxiliary behavior ratios. When built upon HECGCN, our model achieves significant gains in recommending high-quality items (high-ratio group) and maintains a strong advantage in the low-ratio group. This further validates that our method’s ability to mitigate confounders is robust and not limited to a single GCN architecture.

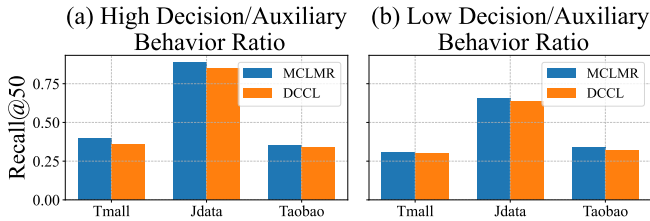


Figure 8: Recall on high and low decision/auxiliary behavior ratio item groups with the HECGCN backbone.

D.2 Analysis with LightGCN Backbone

We further conduct experiments using LightGCN, a simpler yet powerful backbone, to verify our model’s compatibility and effectiveness.

D.2.1 Performance in User Groups. The results, summarized in Figure 9, show a similar pattern. The LightGCN+MCLMR combination surpasses the LightGCN+DCCL baseline across both user segments. The greater relative improvement in the less-active user group highlights our model’s strong synergy with different types of graph neural networks, from complex (CRGCN, HECGCN) to more streamlined ones (LightGCN).

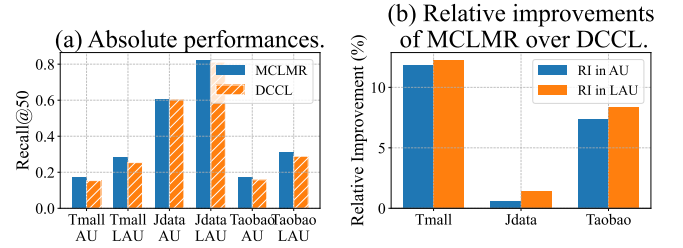


Figure 9: Performance comparison with the LightGCN backbone in active (AU) and less-active (LAU) user groups. (a) Absolute performance; (b) Relative improvements of MCLMR over DCCL.

D.2.2 Recommendation Quality. As depicted in Figure 10, our model continues to excel at identifying high-quality items when paired with LightGCN. It demonstrates superior performance in the high-ratio item group while also performing robustly in the low-ratio group. This consistency across all three backbones provides strong evidence that the improvements stem from our proposed multi-level causal learning framework rather than the specifics of the GCN architecture.

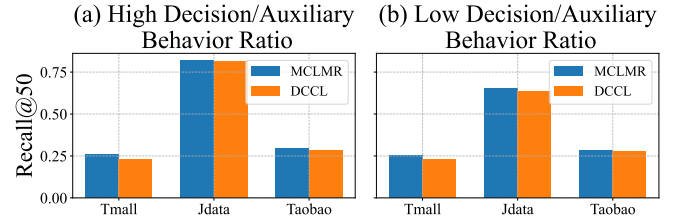


Figure 10: Recall on high and low decision/auxiliary behavior ratio item groups with the LightGCN backbone.

E Time Complexity Derivation

Here, we provide a detailed derivation of the computational complexity introduced by the MCLMR framework and analyze the complexity of baseline models.

E.1 Notations

We define the following symbols for the complexity analysis:

- $N, U, I, E_{\text{total}}$: Total number of nodes ($N = U + I$), users, items, and edges across all behavior graphs.
- d, B, K, k_{exp} : Embedding dimension, behavior types, GCN layers, and MoE experts.
- u_s, b_s : Number of unique users in a batch and the batch size.
- r, L_{max}, H : Avg. Jaccard cost, max sequence length (BCIPM), and hyperedges (HEC-GCN).

E.2 Complexity of MCLMR Modules

The total incremental computational overhead of our framework, O_{MCLMR} , is composed of its three main modules as described in the paper.

Jaccard Aggregation Module: The structural gating path uses Jaccard similarity to measure the overlap between item sets for a user across different behaviors. This calculation is performed for each user and for behaviors, leading to a complexity of $O(N \cdot B^2 \cdot r)$.

MoE Gating Aggregation Module: The semantic gating path employs a Mixture-of-Experts (MoE) network. For each user and each pair of behaviors, the MoE gate processes the embeddings. The complexity is proportional to the number of users, the square of the number of behaviors, the number of experts, and the embedding dimension, resulting in $O(N \cdot B^2 \cdot k_{\text{exp}} \cdot d)$.

Multi-behavior Contrastive Learning Module: The relational alignment is achieved via a contrastive loss calculated over pairs of different behavioral views for each user in a batch. For each of the u_s users in a batch, we compute similarity scores for all $B(B-1)/2$ pairs of behaviors. This results in a complexity per batch of $O(u_s \cdot B^2 \cdot d^2)$. Symmetrically, for each of the i_s unique items in the batch, the item-centric complexity is $O(i_s \cdot B^2 \cdot d^2)$.

Summing the complexities of the components, the total incremental complexity introduced by the MCLMR framework is:

$$O_{\text{MCLMR}} = O(N \cdot B^2 \cdot (r + k_{\text{exp}} \cdot d) + (u_s + i_s) \cdot B^2 \cdot d^2)$$

E.3 Complexity of Backbone Models

The computational complexity of each backbone model is determined by its core architecture and key operations, as detailed below:

(1) CRGCN: The complexity is primarily determined by its graph propagation mechanism. The model employs a cascading structure with L GCN layers for each of the K behaviors. Since graph propagation is the most computationally intensive step, the dominant complexity is driven by it, which is $O(L \cdot E_{\text{total}} \cdot d)$. (2) HEC-GCN: The model’s complexity is composed of three main parts. (1) Graph Convolution: Standard GCN propagation on user-item graphs, with a complexity of $O(L \cdot E_{\text{total}} \cdot d)$. (2) Hypergraph Learning: Operations on the behavior-specific hypergraphs, costing approximately $O(K \cdot (M + N) \cdot S \cdot d)$. (3) Contrastive Learning: The theoretically dominant component, which compares each node against all others, resulting in a complexity of $O(K \cdot (M^2 + N^2) \cdot d)$. In practice, this is often optimized using in-batch negative sampling to $O(K \cdot b^2 \cdot d)$ per batch, where b is the batch size. Thus, the total theoretical complexity is: $O(L \cdot E_{\text{total}} \cdot d + K \cdot (M + N) \cdot S \cdot d + K \cdot (M^2 + N^2) \cdot d)$ (3) BCIPM: The

model’s complexity relies on GCNs for representation learning and a specialized neighborhood aggregation mechanism. The total complexity for graph propagation is approximately $O(L \cdot E_{\text{total}} \cdot d)$. The key computational module is the neighborhood aggregation, which for a batch of b_s users processing padded neighbor lists up to L_{max} , has a complexity of $O(b_s \cdot L_{\text{max}} \cdot d^2)$. Therefore, the final complexity is dominated by these two steps: $O(L \cdot E_{\text{total}} \cdot d + b_s \cdot L_{\text{max}} \cdot d^2)$.

F Empirical Runtime Analysis

To complement the theoretical complexity derivation in Appendix E, we conducted empirical tests to measure the real-world computational overhead and inference latency.

F.1 Experimental Setup

All runtime experiments were conducted on a Linux server equipped with an NVIDIA H20-3e GPU and Intel Xeon CPUs. We measured the average time per training epoch and the total inference time for generating recommendations for all users on the test set.

F.2 Training Overhead

Table 8 compares the training time per epoch of the backbone models with and without MCLMR integration on the Tmall and Taobao datasets.

Table 8: Comparison of average training time (seconds per epoch) on NVIDIA H20-3e GPU.

Method	Tmall		Taobao	
	Original	+MCLMR	Original	+MCLMR
HEC-GCN	625s	650s	502s	579s
CRGCN	145s	182s	110s	135s

The results show that MCLMR introduces a manageable overhead. For complex backbones like HEC-GCN on Tmall, the increase is approximately 4% (625s to 650s). Even for lighter backbones like CRGCN, the absolute time increase is small, validating that our framework is computationally efficient for large-scale training.

F.3 Inference Latency

Crucially, the additional modules in MCLMR (e.g., MoE Gating, Contrastive Learning) are designed to refine the user and item embeddings during the *training phase*.

At the *inference phase*, the recommendation score is computed using the standard inner product of the learned embeddings (Eq. 13 in the main text):

$$\hat{y}_{ui} = e_{u,K_t} \cdot e_{i,K_t}^T$$

This operation is identical to that of the backbone models (e.g., Matrix Factorization or LightGCN style retrieval). Therefore, MCLMR incurs zero additional latency during online inference, making it highly suitable for real-time recommendation scenarios where low latency is critical.